Acta of Bioengineering and Biomechanics
Vol. 18, No. 4, 2016

Original paper
DOI: 10.5277/ABB-00558-2016-02

Numerical investigations of the unsteady blood flow in the end-to-side arteriovenous fistula for hemodialysis

DANIEL JODKO*, DAMIAN OBIDOWSKI, PIOTR REOROWICZ, KRZYSZTOF JÓŹWIK

Lodz University of Technology, Institute of Turbomachinery, Lodz, Poland.

Purpose: The aim of this study was to investigate the blood flow in the end-to-side arteriovenous (a-v) fistula, taking into account its pulsating nature and the patient-specific geometry of blood vessels. Computational Fluid Dynamics (CFD) methods were used for this analysis. *Methods:* DICOM images of the fistula, obtained from the angio-computed tomography, were a source of the data applied to develop a 3D geometrical model of the fistula. The model was meshed, then the ANSYS CFX v. 15.0 code was used to perform simulations of the flow in the vessels under analysis. Mesh independence tests were conducted. The non-Newtonian rheological model of blood and the Shear Stress Transport model of turbulence were employed. Blood vessel walls were assumed to be rigid. *Results:* Flow patterns, velocity fields, the volume flow rate, the wall shear stress (WSS) propagation on particular blood vessel walls were shown versus time. The maximal value of the blood velocity was identified in the anastomosis – the place where the artery is connected to the vein. The flow rate was calculated for all veins receiving blood. *Conclusions:* The blood flow in the geometrically complicated a-v fistula was simulated. The values and oscillations of the WSS are the largest in the anastomosis, much lower in the artery and the lowest in the cephalic vein. A strong influence of the mesh on the results concerning the maximal and area-averaged WSS was shown. The relation between simulations of the pulsating and stationary flow under time-averaged flow conditions was presented.

Key words: *aneurysm, anastomosis, arteriovenous fistula, thrombosis, wall shear stress, intimal hyperplasia*

1. Introduction

Hemodialysis is a treatment for patients suffering from the end-stage renal disease (ESRD). There is a lack of data showing what percentage of the global population suffers from this illness but a number of hemodialysed patients still increases because of ageing of the society [25]. In the hemodialysis process, blood is withdrawn from patient's vascular bed and circulates through a special filter that removes products of metabolism. An arteriovenous fistula (AVF) is a surgically created connection between patient's artery and vein and since 1966 [3] it has been a preferred vascular access for hemodialysis. Once this connection is made, a maturation process of the AVF begins and lasts even a few months depending on a particular patient [7]. During the maturation, high pressure blood from the artery flows directly to the vein and extends its diameter. Finally, the blood flow rate in the vein is even 500 times higher than the normal one, which ensures efficient hemodialysis. However, abnormal hemodynamics associated with a disturbed flow and non-physiological wall shear stress (WSS) leads very often to common vascular complications, e.g., true and false aneurysms, thrombosis, stenosis (narrowings), etc., [4], [5], [24]. Therefore, the AVF is still considered to be an Achilles' heel of hemodialysis and its dysfunctions result in high costs of the treatment. The primary reasons of AVF dysfunctions are sought among flow phenomena, because it is thought that functioning of the fistula is above all a hydraulic problem.

* Corresponding author: Daniel Jodko, Lodz University of Technology, Institute of Turbomachinery, ul. Wolczanska 219/223, 90-924 Lodz, Poland, Tel: +48 42 631 23 64, fax: +48 42 631 24 78, e-mail: daniel.jodko@p.lodz.pl

Received: January 26th, 2016
Accepted for publication: March 29th, 2016

2. Materials and methods

Geometrical model

The reconstruction method of the blood vessels was shown in [10], [22]. DICOM images of the matured end-to-side radiocephalic a-v fistula were obtained from the angio-computed tomography, 12 weeks after the connection had been created. Projections were done every 0.3 mm. Images were used as a source of geometrical data and applied to develop a 3D CAD model of the fistula. The DICOM files were imported into an RSR2 medical image viewer, in which blood vessels are visualized as circular or oval shapes in particular 'slices' of patient's forearm. The RSR2 enables one to read coordinates of the points located in the centre of the blood vessel section. These coordinates are saved in a text file that can be loaded to Solid Works 2012 in order to draw a 3D curve in the Cartesian system of coordinates. Moreover, dimensions of the observed anatomical structures can be measured with the RSR2 viewer. The normal artery is considered to have a circular cross-section, thus if the blood vessel section is oval, its smaller diameter is assumed to represent a real diameter of the blood vessel. The data were collected from the subsequent 10–50 cross-sections of the forearm (every 3–15 mm along the *z* axis), thus providing the full information on the 3D course of blood vessels as well as their variable lumen size. Partially, for the most complicated zones, the model was segmented. The complete 3D CAD model of the patient-specific fistula was built in Solid Works (see Fig. 1). The model was imported to the Design Modeler, which is a part of ANSYS (v. 15.0) Workbench. The model represents a volume of the blood flowing through the fistula and its external walls are internal walls of blood vessels.

A few characteristic regions of the fistula: a radial artery, a cephalic vein that is cannulated in hemodialysis, and an anastomosis were distinguished. The anastomosis was divided into five parts (Fig. 2).

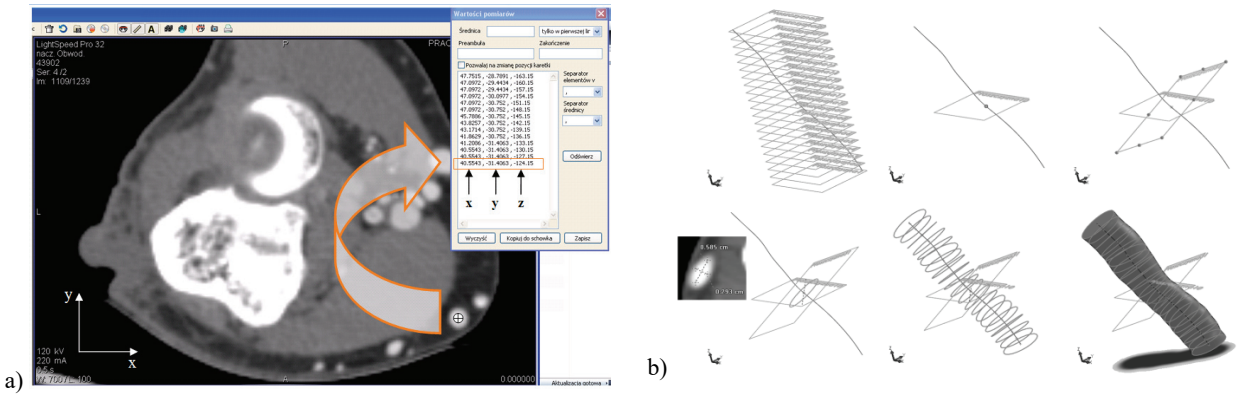

Fig. 1. (a) One particular projection of the forearm observed in the RSR2; (b) Subsequent steps of the blood vessel formation

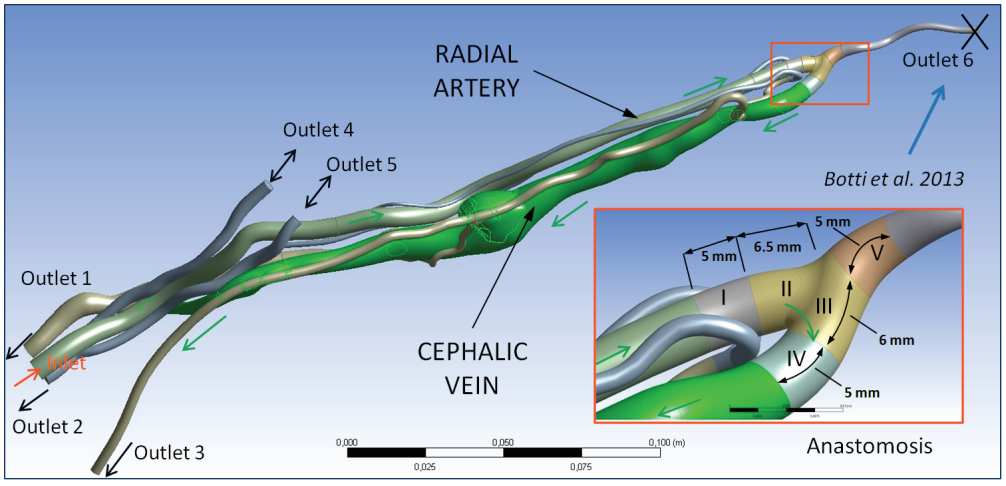

Fig. 2. Fistula with distinguished regions monitored in ANSYS 15.0

Assumptions and boundary conditions

Blood is considered to be a non-Newtonian fluid and its dynamic viscosity depends on the shear rate (strain, velocity gradient). The dynamic viscosity is related to local flow conditions, which is confirmed by experiments [23]. In the literature, numerous mathematical rheological models of blood can be found. Some of them define the blood viscosity not only as a function of the shear rate but also take into account other patient-specific parameters (hematocrit, total protein minus albumin (TPMA) concentration, etc.) [12], [19]. In the simplest mathematical model, blood can be assumed to be a Newtonian fluid with constant dynamic viscosity but this is valid only in the case of the flow characterized by high Reynolds numbers that usually occur in large arteries or the anastomosis. In this study, various blood vessels of different internal diameters and flow conditions were taken into account. High values of the shear rate in the anastomosis area and very low values of this parameter in veins were expected. Thus, in these investigations, a modification of the Power Law model, with the dynamic blood viscosity (η) defined as

$$\begin{cases} \eta = 0.55471 & \text{for } \dfrac{\partial V}{\partial y} < 10^{-3} \\ \eta - \eta_0 \left(\dfrac{\partial V}{\partial y} \right)^{n-1} & \text{for } 10^{-3} \le \dfrac{\partial V}{\partial y} < 327 \\ \eta = 0.00345 & \text{for } \dfrac{\partial V}{\partial y} \ge 327 \end{cases} \quad (1)$$

where η_0 = 0.035 Pa s, n = 0.6, and $\dfrac{\partial V}{\partial y} s^{-1}$ is the shear rate, was used. This model was employed as its quality had been proven in [10], [11], [13], [20], [22].

In the present study, a constant value of blood density equal to 1040 kg/m^3 was assumed, which is slightly lower than the typical arterial blood density [14].

The Prandtl velocity profile with an exponent equal to 0.167, typical of turbulent flows in cylindrical channels and low values of the Reynolds number, was introduced as the boundary condition at the inlet cross-section [11]. The maximal blood velocity V_{max} is located in the centre of the inlet and varies with time. The time-dependent maximal velocity waveform is shown in Fig. 3 (time-averaged value of the V_{max} is equal to 0.645 m/s). Typical parameters characterizing this single-phase flow were calculated, i.e., a pulsatility index (PI = 0.77), a resistance index (RI = 0.53), and a systolic-diastolic velocity ratio (SD = 2.14). The static pressure waveform (Fig. 3) characteristic of the subclavian artery but three times smaller due to a large pressure drop was used as the boundary condition at all outlet cross-sections with the time-averaged value equal to 4335 Pa [20]. The peak value of pressure is offset by 0.1 s from the maximal velocity. The distal artery usually receives a very inconsiderable amount of blood or even an inflow may be observed in this place (steal syndrome). Thus, similarly to Botti [2], Outlet 6 was assumed to be clamped with the wall condition. One single cardiac cycle lasts 0.84 s, which corresponds to approx. 71.4 bpm of the heart operation. Three cardiac cycles were considered in this study. The reference pressure of 101 325 Pa was defined. A few values of the timestep were compared and, finally, Δt = 0.005 s yielding a stable solution was chosen and used. The convergence criterion lower than 10^{-4} was achieved for mass and momentum. No heat transfer was considered.

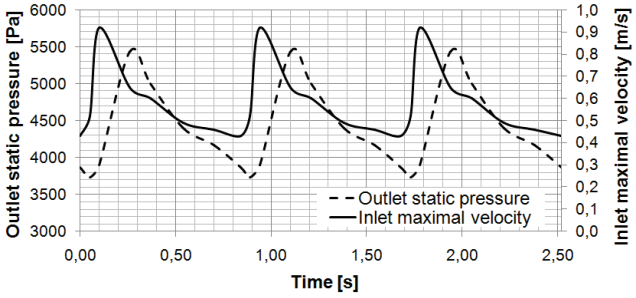

Fig. 3. Maximal blood velocity waveform [m/s] and the static pressure waveform [Pa] used as the boundary conditions for the inlet cross-section and outlet cross-sections, respectively

In the present study, elasticity of blood vessel walls is neglected. However, according to other authors [6], [17], this approach is still reasonable and gives the results even 12 times faster than Fluid Structure Interaction simulations.

Solution

The ANSYS CFX v.15.0 commercial code was used to conduct necessary calculations [1]. Additionally, the shear stress transport (SST) model of turbulence with automatic wall treatment, which combines the k–ω and k–ε turbulence models, was applied. However, for low values of y^+, obtained in this case, the flow was fully solved in the vicinity of walls.

Mesh independence tests

A mesh independence test was performed. For this purpose, the steady flow simulations, in which

end-systolic blood flow conditions were used as the boundary conditions, were conducted. The highest velocity gradients occur under these conditions, thus the worst possible situation was considered in the test. Some selected flow parameters obtained from the results were compared. All of them were confronted for various meshes, differing in a number of sublayers in the boundary layer. The constant total thickness (0.8 mm) of the boundary layer was assumed for all the cases under investigation.

Hence, the difference between the results obtained for two subsequent meshes was calculated as

$$E = \frac{R_{ii} - R_i}{R_{ii}} \cdot 100\%, \tag{2}$$

where E – difference [%], R_{ii} – parameter obtained from the results for the finer mesh, and R_i – parameter obtained from the results for the coarser mesh.

The parameters which were compared during the mesh independence test are as follows: the maximal WSS in the anastomosis (that occurs in Region II, Fig. 2), the area-averaged WSS (AAWSS) in Region II, the AAWSS in the radial artery, the AAWSS in the cannulated cephalic vein, the maximal blood velocity

Table 1. Comparison of the parameters obtained from the steady flow simulations performed in the mesh independence test

MESH parameters					Max y^+	Flow parameters obtained from the steady flow simulations					
NFV	NN	NLW	AS	MTBL		Max WSS II	AAWSS II	AAWSS V	AAWSS A	Max Vel	FR
[million]		[–]	[–]	[mm]	[–]	[Pa]				[m/s]	[cm^3/s]
7.29	2.86	10	0.251	0.80	3.60	200.7	22.58	5.337	12.031	2.736	24.375
8.20	3.32	12	0.245		2.54	233.6	24.57	5.708	12.356	2.640	24.395
9.11	3.77	14	0.239		1.78	256.2	26.12	5.872	12.576	2.659	24.404
10.02	4.23	16	0.235		1.26	275.3	27.23	5.963	12.726	2.691	24.411
10.94	4.69	18	0.230		0.89	292.0	28.01	6.038	12.825	2.668	24.414
11.85	5.15	20	0.226		0.62	304.7	28.56	6.087	12.894	2.641	24.424
12.76	5.61	22	0.223		0.43	314.1	28.97	6.115	12.934	2.694	24.423
13.68	6.06	24	0.220		0.34	319.4	29.22	6.126	12.976	2.691	24.422

NFV – number of finite volumes, NN – number of nodes, NLW – number of layers near the wall, AS – average Skewness, MTBL – maximal total thickness of the boundary layer, Max WSS II – maximal WSS in Region II, AAWSS II – area-averaged WSS in Region II, AAWSS V – area-averaged WSS in the cannulated vein, AAWSS A – area-averaged WSS in the radial artery, Max Vel – maximal blood velocity in the whole domain, FR – volume flow rate at Outlet 1.

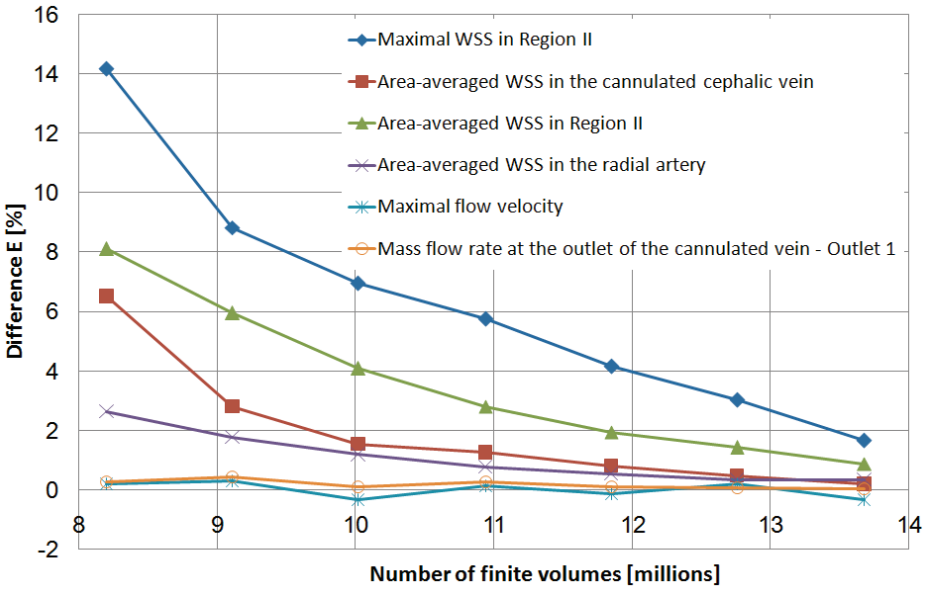

Fig. 4. Differences calculated for the examined meshes in the mesh independence test

in the domain (that was found in the anastomosis), and the mass flow rate at Outlet 1, which is the cephalic vein outlet. A comparison of the parameters obtained and the differences calculated for the test meshes are shown in Table 1 and in Fig. 4, respectively. The maximal value of the WSS is observed only in the limited region and it can be considered as a local phenomenon. On the basis of this, it is assumed that the difference calculated for the maximal value of the WSS cannot be higher than 2%. However, other parameters that were taken into account in the mesh independence test have a global range. In those cases, it was assumed that the absolute value of the maximal differences in the observed parameters should not exceed 1%.

Additionally, one of the mesh quality measures referred to as *Skewness* was compared for each generated mesh. According to the ANSYS Meshing User's Guide [1], *Skewness* is defined as a difference in the optimal cell size and the created cell size divided by the optimal cell size. The lower the parameter value, the higher the quality of the examined mesh. According to the ANSYS instructions, the mesh elements characterized by *Skewness* lower than 0.250 are considered to be excellent.

When the differences reached the acceptable level, the densest mesh was assumed to be satisfactory for simulations of the unsteady state. Finally, a mesh consisting of 13.68 million finite volumes, 6.06 million nodes and 24 sublayers of prismatic elements representing the boundary layer of the maximal total thickness equal to 0.8 mm was used for the further investigations related to the pulsating blood flow. Moreover, the results obtained from the steady state simulations, performed for this mesh, were used as initial conditions in the simulation of the unsteady flow. The analysis of the obtained y^+ parameter values allows one to conclude that the flow is fully solved in the boundary layer despite the assumption of the automatic wall function.

3. Results

Flow

Some points at specific positions of vessels were selected to monitor velocity values throughout the whole simulation process. The monitoring points were placed in the centres of vessels and their locations are presented in Fig. 5. The results of velocity monitoring at the defined points are depicted in Fig. 6. The line A, identical to the waveform from Fig. 3, is the maximal blood velocity waveform observed in the centre of the inlet cross-section. As one can notice, this is a regular curve without oscillations with one maximal and one minimal peak value equal to 0.92 m/s and 0.43 m/s, respectively. The velocity increases at the point B that is located in the artery 50 mm upstream of the anastomosis, and it still changes its form, following the inlet condition definition. The initial oscillations can be recognized at the curve C obtained for the point which is placed 25 mm upstream of the anastomosis. The next few lines denoted as D-H describe the blood velocity in anastomosis regions. In these cases, more oscillations of the velocity, which indicate an occurrence of the transitional flow, can be observed. Such a disturbed flow in the anastomosis zone was also described in [8], [9]. At the points that are placed downstream of the anastomosis (I and J), the oscillations are still observed. At point K located inside the aneurysm formed in the cannulated vein, the blood velocity changes in an irregular way during three

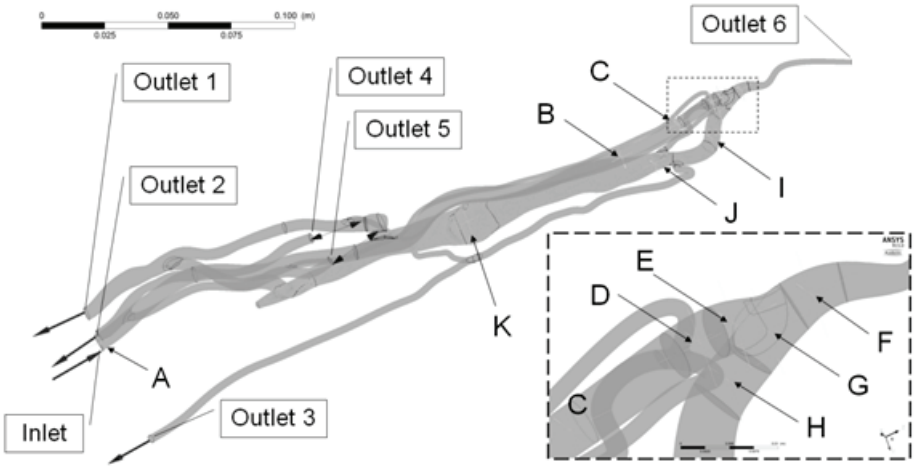

Fig. 5. Localization of the points in which the blood velocity was monitored

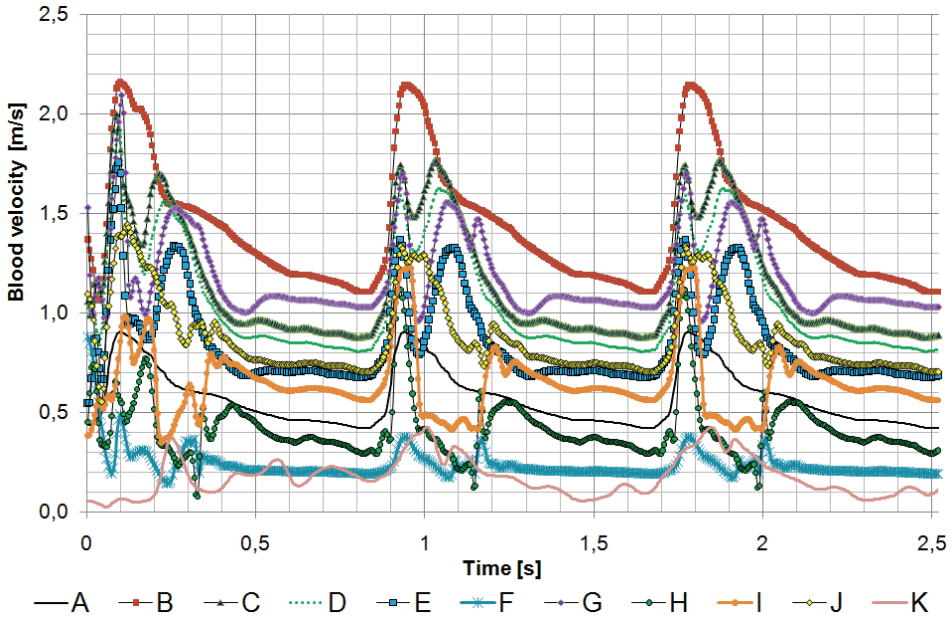

Fig. 6. Resultant blood velocity versus time monitored during the simulation of the unsteady flow at particular points defined in Fig. 5

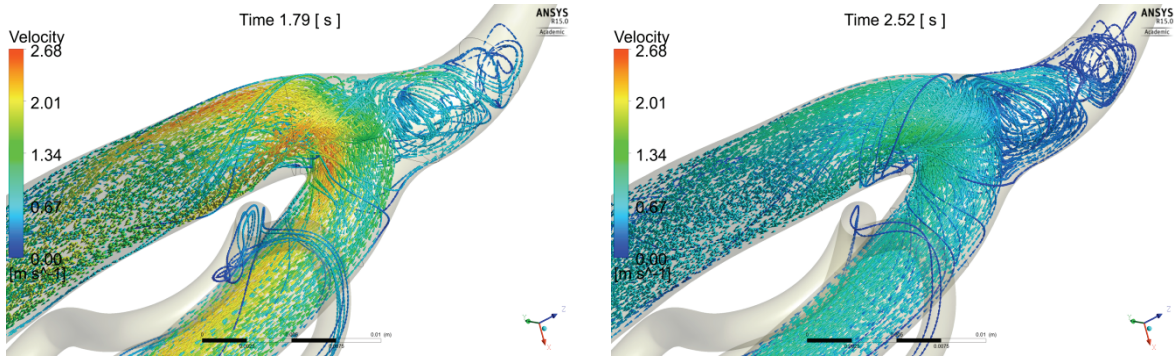

Fig. 7. Resultant velocity and blood flow patterns observed for two timesteps around the anastomosis

Table 2. Comparison of the mean volume flow rate (minus means an outflow) and its percentage calculated for the outlets and the inlet

Volume flow rate	Inlet	Outlets					
		1	2	3	4	5	6
[cm^3/s]	18.31	–15.84	–0.048	–2.12	–0.0024	–0.30	0
[l/min]	1.098	–0.9503	–0.0029	–0.13	–0.00014	–0.018	0
[%]	100.00	86.52	0.26	11.55	0.01	1.66	0

cardiac cycles with low oscillations and low average values. The maximal value of the blood velocity, equal to 2.68 m/s, was found in the anastomosis region at the timestep 1.79 s (Fig. 7). The blood flow is animated and presented in the Supplementary materials (S1-S3).

Figure 6 shows inertial effects occurring during the first cardiac cycle. The third cycle is almost the same as the second one, therefore, further results will be given for the third period of the heart operation to minimize an influence of initial conditions onto the flow analysis results. The flow rate at the outlet cross-sections, blood velocity and flow patterns obtained for the third cardiac cycle (t = 1.69–2.52 s) were analysed at particular characteristic timesteps (e.g., peak systole, late diastole) and as time-averaged parameters.

The time-averaged volumetric flow rate, calculated for the inlet and outlet cross-sections, is presented in Table 2. The highest value of the outflow (86.5%) is observed in the cannulated vein (Outlet 1),

which is expected in the correctly functioning fistula. A smaller amount of blood received by the cephalic vein was obtained in [17], both in rigid-wall (68%) and FSI (70%) simulations.

Wall shear stress

One has to remember that the WSS is a complex function dependent on blood viscosity and strain, according to Newton's law

$$WSS = \eta \frac{\partial V}{\partial y}. \tag{3}$$

A decrease in the shear strain $\frac{\partial V}{\partial y}$ is associated with an increase in the blood dynamic viscosity η, thus the WSS is strongly dependent on local flow conditions. Figure 8 and the Supplementary material S4 depict the dynamic viscosity of blood versus the location and time. Changes in the shear strain are animated in the Supplementary material S5.

Changes in the maximal WSS values in particular regions defined in Fig. 2 are depicted in Fig. 9a. The WSS reaches the highest values in Region II, very close to the place where the vein is sutured to the ar-

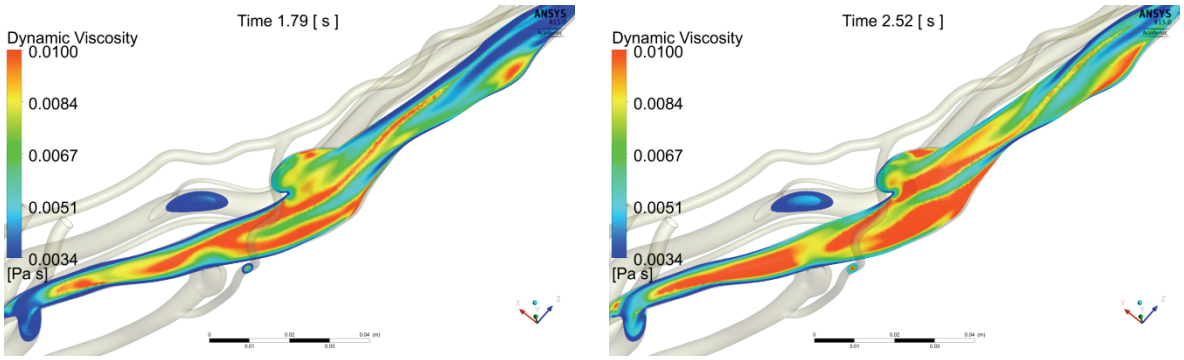

Fig. 8. Distribution of the blood dynamic viscosity on the plane passing through the aneurysm in two timesteps

Table 3. Comparison of time-averaged values of the max. WSS and time-averaged values of the area-averaged WSS in particular regions of the fistula obtained from the non-stationary simulations

Parameter	Region						
	Radial artery	Anastomosis					Cephalic vein
		1	2	3	4	5	
Max WSS averaged over time [Pa]	40.35	16.20	163.26	97.55	79.63	34.11	40.32
		Average: 78.15					
AAWSS averaged over time [Pa]	**7.02**	7.34	15.61	31.40	23.30	5.90	**3.02**
		Average: 16.71					

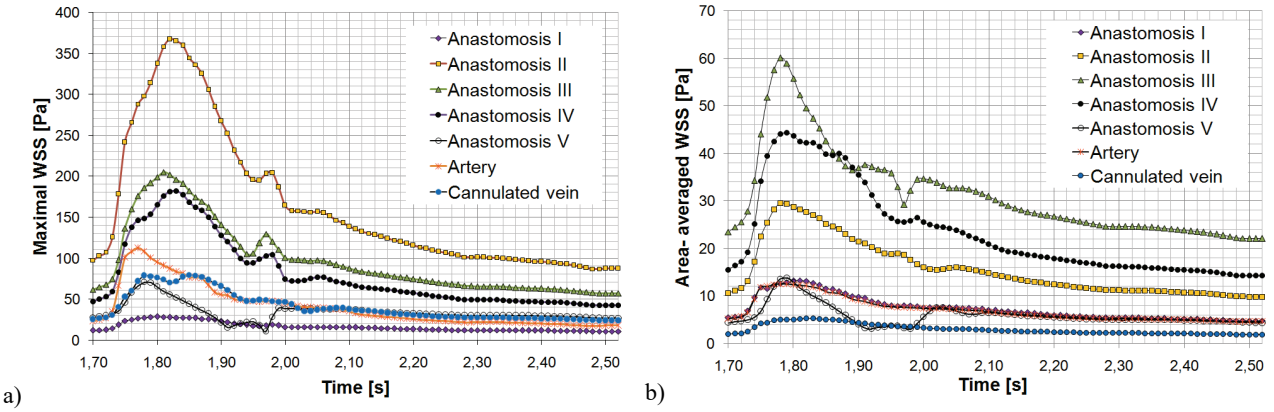

a) b)

Fig. 9. Changes in the maximal WSS values (a) and the area-averaged WSS (b) in particular regions of the fistula obtained for the third cardiac cycle

tery. However, the extremely high WSS appears only locally, which has already been mentioned. It is worth noticing that the AAWSS (Fig. 9b) is not the greatest in Region II, despite the occurrence of an extremely high WSS. The highest values of the AAWSS were found in Region III. The maximal WSS and the AAWSS were also averaged over time (Table 3). Both parameters are higher in the feeding artery than in the cephalic vein, and extremely high in the anastomosis. The Supplementary materials S6–S8 present a distribution of the WSS versus time. In particular regions in the vicinity of the anastomosis, WSS values are permanently higher than 20 Pa, which is marked with the red colour on the scale.

Simulations with time-averaged parameters as the boundary conditions

Finally, a stationary simulation of the flow was carried out, in which the time-averaged volume flow rate obtained from the non-stationary simulations at the inlet cross-section (18.31 cm^3/s) and the time-averaged static pressure at the outlets (4335 Pa) were used. The aim of that part of the study was to compare the results obtained from those simulations to the time-averaged results of the non-stationary experiment. In this case, the largest mesh obtained in the independence test was used. All other assumptions were the same as described earlier, except for the fact

Table 4. Results obtained from the simulation of the steady-state blood flow, in which the time-averaged mass flow rate and pressure were employed as the boundary conditions

Parameter	Region						
	Artery	Anastomosis					Cephalic vein
		1	2	3	4	5	
Max. WSS [Pa]	36.80	14.82	151.8	96.68	77.79	33.24	37.67
		Average: 74.87					
AAWSS [Pa]	**6.97**	7.06	15.09	31.35	23.69	5.54	**2.96**
		Average: 16.55					
Volume flow rate [l/min]	1.098 (Input parameter at Inlet)	–					–0.9505 (Outlet 1)

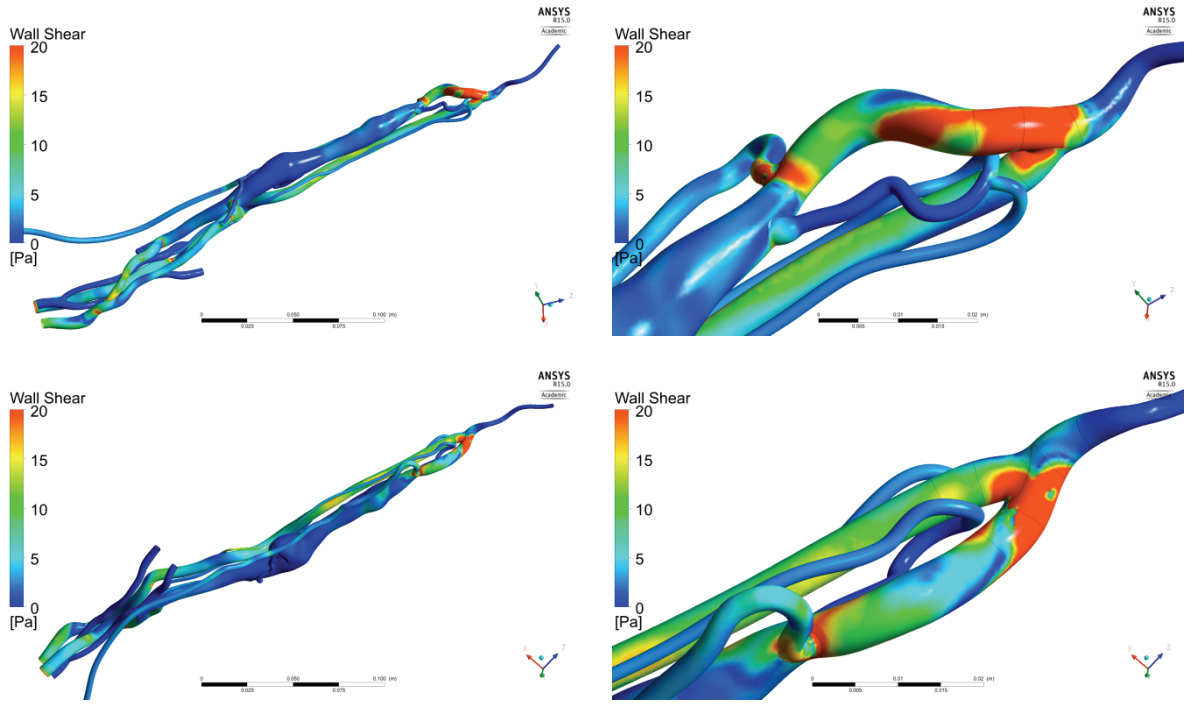

Fig. 10. Wall shear stress [Pa] distribution in the whole domain and around the anastomosis – the results were obtained from the simulation of the steady-state blood flow, in which the time-averaged mass flow rate and pressure were employed as the boundary conditions – the red colour denotes the WSS equal to or higher than 20 Pa

that the Prandtl profile at the inlet was not used. Nevertheless, the velocity profile was fully formed before the anastomosis due to the length of the supplying artery. In this case, the maximal value of the blood velocity, equal to 1.74 m/s, was found in the anastomosis. The maximal value of y^+ was equal to 0.42. The AAWSS (Table 4) calculated for the artery (6.97 Pa), the cephalic vein (2.96 Pa) and the whole anastomosis (16.55 Pa) are close to the time-averaged AAWSS extracted from the non-stationary simulation results as illustrated in Table 3. The results related to the WSS distribution are shown in Fig. 10, where the red colour denotes the WSS ≥ 20 Pa. Such an extremely high WSS occurs in the anastomosis and around branching regions.

4. Discussion

The aim of this study was to carry out simulations of the pulsating blood flow through the native patient-specific end-to-side arteriovenous fistula, in which a complex structure of blood vessels was taken into account. The study confirms an occurrence of the disturbed blood flow in the anastomosis and extremely high values of the blood velocity in this region (2.68 m/s). Disturbances take place despite low values of the Reynolds number that changes in the range 326–869 (484 on average) at the inlet cross-section (based on the averaged flow rate and the area-averaged dynamic viscosity calculated at the inlet in particular timesteps). The mean volume flow rate of blood, calculated for the outlet of the cephalic vein, reaches the level of 15.8 cm^3/s (0.95 l/min), which is higher than the minimal flow rate ensuring sufficient hemodialysis > 5.83–6.67 cm^3/s (0.35–0.40 l/min) [16]. In fact, this fistula was assessed to be useful for treatment by physicians.

The mesh precision in the vicinity of the wall plays a key role in the determination of the WSS. This study presents an influence of the number of sublayers created in the boundary layer on the maximal and area-averaged WSS in particular regions of the fistula. The AAWSS seems to be a better parameter to indicate the utility of the mesh, because the maximal WSS occurs only locally and is much more strongly dependent on the local geometry and the mesh quality in the vicinity of the wall. This is a very important part of these investigations which has not been so deeply investigated in our previous paper [10] and anywhere else.

The WSS distribution was determined and its maximal and area-averaged values versus time were shown. It provides the information on the amplitudes of changes in those parameters that are high in the anastomosis and relatively low in the radial artery and the cephalic vein. Those parameters were averaged over time. The time-averaged AAWSS reaches the highest value in the whole anastomosis (16.71 Pa) with the maximal value in Region III. Values higher than 10–15 Pa are thought to be non-physiological. Although the time-averaged AAWSS in the cephalic vein is relatively low (3.02 Pa), it is not extremely low (WSS < 1 Pa). The highest values of the WSS occur in a more distal part of the vein, close to the anastomosis. It is considered that a division of the vein region into smaller regions (analogous to the anastomotic area) would result in detection of lower values of the time-averaged AAWSS in more proximal parts, especially at the aneurysm area, in which the blood velocity is very low and even a reverse flow occurs. The low WSS, related to the occurrence of low blood velocities, may result in the thrombus deposition on the inner wall of the cannulated cephalic vein [4], [5]. Despite the fact that in the literature there are numerous methods used for the extraction of the WSS in numerical investigations, a similar distribution of the WSS is reported by other researchers [6], [8], [15], [18]. However, this study shows a new method of quantitative assessment of the WSS in particular regions of the shunt.

The simulations, for which the time-averaged flow rate and pressure were used as the boundary conditions, yield comparable results to the time-averaged ones obtained from the simulations of the unsteady flow. This novel and important finding may be employed if the computational methods are adopted in clinical practise. The simulations show that this approach is reasonable and allows one to reduce significantly the simulation time. The time needed for carrying out the unsteady state simulations reached 11 days and 9 hours, whereas the stationary simulations with time-averaged boundary conditions took 15 hours only. The same computer was used in both cases (Intel Core i7-3930K 3.20GHz, 8 cores, 64.0 GB RAM), thus the difference is considerable.

5. Conclusions

The blood flow through an arteriovenous fistula is fascinating and not fully understood yet, however an influence of local flow conditions on the development of complications is apparent and confirmed by other researchers. This study shows a disturbed blood flow

in the a-v fistula that may be a reason of oscillations of the flow velocity and, consequently, the wall shear stress, especially in the anastomosis territory. These phenomena are thought to play a key role in the proliferation of endothelial cells that results in further complications. Moreover, high gradients of the blood velocity and its local oscillations can induce blood platelets activation in the anastomosis and further thrombus deposition in the cannulated cephalic vein, in which blood velocity is relatively low [5].

A non-physiological WSS, i.e., very low (lower than 1 Pa), extremely high (higher than 10–15 Pa) or highly oscillating, can induce a biological answer which was interestingly explained in [4], [5]. The shear force affects the endothelial surface, however this mechanical factor is also transmitted by the cytoskeleton to the endothelial basal layer.

In this study, elasticity of blood vessel walls was neglected. According to [6], [17], in which the authors compare the results obtained from CFD and FSI simulations, one can state that the obtained quantitative results related to the WSS are overestimated in particular regions of the fistula. If such an error exists, there is a risk of occurrence of a much lower WSS in the cannulated vein, but the anastomosis would not be affected by so high and dangerous shear force as presented in this study. An intense WSS occurs in the anastomosis, which may be a reason of intimal hyperplasia and adverse remodelling of the wall. On the other hand, the results of the CFD simulation allow one to observe a relative magnitude and a range of oscillations of the WSS in particular regions of the fistula much faster than the FSI approach [6].

The proposed method for distinguishing fistula regions and spatial averaging of the WSS seems to be a good way to show an influence of the distance from the anastomosis on the WSS magnitude. The study focuses only on the anastomosis region, in which abnormal phenomena are expected, however the cannulated vein can also be divided into smaller parts. We believe that CFD methods can be useful in prediction of occurrence of fistula complications, however longer monitoring of the fistula is necessary.

Furthermore, it has to be remembered that in the case of a blood flow through the fistula, the problem of time scale selection is to be faced. Only one particular cardiac cycle can be taken into account, but when the fistula behaviour is considered for a longer time, then time-averaged parameters can be analysed. This study shows that an application of time-averaged parameters as boundary conditions is well-founded.

Finally, great efforts involving CFD methods have been undertaken over the years in order to find the reasons of fistula failures. The authors of the present study believe that computational methods may also be helpful in the maintenance of a-v fistulas because these methods allow one to gain the majority of information, which is not available from the Colour Doppler ultrasound imaging [21].

Supplementary materials can be found at the website: http://figshare.com

Acknowledgments

We would like to thank Radosław Pietura, MD, and his colleagues from Medical University of Lublin, Poland, for the medical data used to develop a 3D-CAD model of the fistula. We also thank Ms Małgorzata Jóźwik for her significant help during the preparation of the manuscript.

Financial Support: This project was financially supported by the Fund for Young Scientists granted by the Faculty of Mechanical Engineering, Lodz University of Technology, and Preludium 7 granted by the National Science Centre in Poland (2014/13/N/ST8/04031).

Conflict of Interests: None

References

[1] ANSYS CFX Theory & Meshing User's Guide. ANSYS Release 15.0 ANSYS Inc.

[2] BOTTI L., CANNEYT K.V., KAMINSKY R., CLAESSENS T., PLANKEN R.N., VERDONCK P., REMUZZI A., ANTIGA L., *Numerical Evaluation and Experimental Validation of Pressure Drops Across a Patient-Specific Model of Vascular Access for Hemodialysis*, Cardiovasc. Eng. Technol., 2013, 4(4), 485–499.

[3] BRESCIA M.J., CIMINO J.E., APPEL K., HURWICH B.J., *Chronic hemodialysis using venipuncture and a surgically created arteriovenous fistula*, N. Engl. J. Med., 1966, 275(20), 1089–1092.

[4] CHATZIZISIS Y.S., COSCUN A.U., JONAS M., EDELMAN E.R., FELDMAN C.L., STONE P.H., *Role of Endothelial Shear Stress in the Natural History of Coronary Atherosclerosis and Vascular Remodeling*, Journal Am. Coll. Cardiol., 2007, 49(25), 2379–2393.

[5] CHIU J.-J., CHIEN S., *Effects of Disturbed Flow on Vascular Endothelium: Pathophysiological Basis and Clinical Perspectives*, Physiol. Rev., 2011, 91, 327–387.

[6] DECORATO I., KHARBOUTLY Z., VASSALLO T., PENROSE J., LEGALLAIS C., SALSAC A.-V., *Numerical simulation of the fluid structure interactions in a compliant patient-specific arteriovenous fistula*, Int. J. Numer Meth. Biomed. Enging., 2014, 30(2), 143–159.

[7] DIXON B.S., *Why don't fistulas mature?* Kidney International, 2006, 70, 1413–1422.

[8] ENE-IORDACHE B., CATTANEO L., DUBINI G., REMUZZI A., *Effect of anastomosis angle on the localization of disturbed flow in 'side-to-end' fistulae for haemodialysis access*, Nephrol. Dial. Transplant., 2013, 28, 997–1005.

[9] ENE-IORDACHE B., REMUZZI A., *Disturbed flow in radial-cephalic arteriovenous fistulae for haemodialysis: low and oscillating shear stress locates the sites of stenosis*, Nephrol. Dial. Transplant., 2012, 27, 358–368.

[10] JODKO D., OBIDOWSKI D., REOROWICZ P., JÓŹWIK K., *Simulations of the blood flow in the arterio-venous fistula for haemodialysis*, Acta Bioeng. Biomech., 2014, 16(1), 69–74.

[11] JODKO D., OBIDOWSKI D., REOROWICZ P., KŁOSIŃSKI P., JÓŹWIK K., *Angular position determination of heart valves in the pediatric Ventricular Assist Device with use of Computational Fluid Dynamics*, Aktualne Problemy Biomechaniki, 2014, 8, 57–62.

[12] JOHNSTON B.M., JOHNSTON P.R., CORNEY S., KILPATRICK D., *Non-Newtonian blood flow in human right coronary arteries: steady state simulations*, J. Biomech., 2004, 37, 709–720.

[13] JÓŹWIK K., OBIDOWSKI D., *Numerical simulations of the blood flow through vertebral arteries*, J. Biomech., 2010, 43, 177–185.

[14] KENNER T., *The measurement of blood density and its meaning*, Basic Res. Cardiol., 1989, 84, 111–124.

[15] KHARBOUTLY Z., DEPLANO V., BERTRAND E., LEGALLAIS C., *Numerical and experimental study of blood flow through a patient-specific arteriovenous fistula used for hemodialysis*, Medical Engineering & Physics, 2010, 32(2), 111–118.

[16] KONNER K., NONNAST-DANIEL B., RITZ E., *The Arteriovenous Fistula*, J. Am. Soc. Nephrol., 2003, 14, 1669–1680.

[17] MCGAH P.M., LEOTTA D.F., BEACH K.W., ALISEDA A., *Effects of wall distensibility in hemodynamic simulations of an arteriovenous fistula*, Biomech. Model Mechanobiol., 2014, 13, 679–695.

[18] MCGAH P.M., LEOTTA D.F., BEACH K.W., ZIERLER R.E., ALISEDA A., *Restoration of Homeostatic Shear Stress within Arteriovenous Fistulae*, J. Biomech. Eng., 2013, 135(1), 51–59.

[19] MOORE S., *Computational 3D Modelling of Hemodynamics in the Circle of Willis*, University of Canterbury, PhD Dissertation 2007.

[20] OBIDOWSKI D., *Blood flow simulation through human vertebral arteries*, Łódź University of Technology, PhD Dissertation (in Polish) 2011.

[21] PIETURA R., JANCZAREK M., ZAŁUSKA W. et al., *Colour Doppler ultrasound assessment of well-functioning mature arteriovenous fistulas for haemodialysis access*, Eur. J. Radiol., 2005, 55(1), 113–119.

[22] REOROWICZ P., OBIDOWSKI D., KŁOSIŃSKI P., SZUBERT W., STEFAŃCZYK L., JÓŹWIK K., *Numerical simulations of the blood flow in the patient-specific arterial cerebral circle region*, J. Biomech.. 2014, 47, 1642–1651.

[23] SHIN S., KEUM DO-Y., *Measurement of blood viscosity using mass-detecting sensor*, J. Biomech., 2002, 17, 383–388.

[24] SIVANESAN S., HOW T.V., BLACK R.A., BAKRAN A., *Flow patterns in the radiocephalic arteriovenous fistula: an in vitro study*, J. Biomech., 1999, 32, 915–925.

[25] U.S. Renal Data System Technical Report, "2014 USRDS Annual Data Report Volume 2: End-Stage Renal Disease". Washington Heights.